MODELING SOLAR LYMAN ALPHA IRRADIANCE

J.Pap, H.S.Hudson, G.J.Rottman, R.C.Willson, R.F.Donnelly, and J.London

Univ. of Colorado (CIRES)/NOAA, Boulder CO 80309; Univ. of California, San Diego CA 92109; Univ. of Colorado (LASP), Boulder CO 80309; Jet Propulsion Laboratory, Pasadena CA 91103; NOAA/SEL, Boulder CO 80303; Univ. of Colorado (APAS), Boulder CO 80309

ABSTRACT

Solar Lyman alpha irradiance is estimated from various solar indices using linear regression analyses. Models developed with multiple linear regression analysis, including daily values and 81-day running means of solar indices, predict reasonably well both the short- and long-term variations observed in Lyman alpha. It is shown that the full disk equivalent width of the He line at 1083 nm offers the best proxy for Lyman alpha, and that the total irradiance corrected for sunspot effect also has a high correlation with Lyman alpha.

INTRODUCTION

For the first time, the total and UV solar irradiances have been measured simultaneously from space during most of a solar cycle. This permits the quantitative study of irradiance variabilities related to the solar cycle. Lean[1] has shown that variations of UV irradiance are mainly caused by the bright magnetic elements on the solar surface associated with plages and the "active network". A recent study by Barth et al.[2] has shown that variations of Lyman alpha can be modeled reasonably well during the declining portion of solar cycle 21 with the 10.7 cm radio flux, but a phase-shift between the time of their respective solar minimum is evident. In this paper we have used statistical methods to examine the variations of Lyman alpha irradiance and its relation to the total solar irradiance and various ground based solar activity indices.

This paper uses observations of Lyman alpha (121.6 nm) from the Solar Mesosphere Explorer satellite (e.g. Barth et al.[2]). Data for the total solar irradiance (S) come from the SMM/ACRIM radiometer (e.g. Willson[3]). In order to compare the variations of Lyman alpha and total irradiance, the effect of sunspots has been removed from S. For this purpose, the "Photometric Sunspot Index (PSI)", developed by Hudson et al.[4], has been used. The total irradiance corrected for sunspot darkening (Sc) is therefore calculated as Sc=ACRIM+PSI. The 10.7 cm radio flux (F10), Fe XIV coronal green line index (CI), Ca-K plage index (PI), the full disk equivalent width of the He line at 1083 nm (EWHe) and projected sunspot areas (PSSA) are used as indices of solar activity. Daily values of F10 and PI have been published in Solar Geophysical Data catalogue. The Fe XIV coronal index has been calculated from ground-based observations and published through 1986 by Rybansky et al.[5] These data give the total radiant energy of the coronal emission line at 530.3 nm and its variation is known to be controlled mainly by solar magnetic activity, as has been shown by Rybansky et al.[5] The He 1083 nm line equivalent width is measured at the Kitt Peak National Solar Observatory and Harvey[6] has found that it correlates well with the full disk Ca-K index. Thus, it is used as a proxy for the emission of bright magnetic elements, including faculae and the active network. Data sets for projected sunspot areas of "active" and "passive" sunspot groups were created using information on age and magnetic structure of sunspots reported in Solar Geophysical Data catalogue and daily area of spots reported

in Solnechnye Dannye catalogue. The active sunspot groups are defined by Pap[7] as developing complex groups, and the passive groups are the decaying old sunspots. Note that there is no direct physical relationship between the projected sunspot areas and Lyman alpha variability, since changes in Lyman alpha are primarily associated with bright plages and not with sunspots. The projected areas of active and passive spots provide a reliable discriminator of solar activity, indicating the presence of young and old active regions. Therefore we consider the relation of Lyman alpha to both types of sunspots in order to improve our understanding of the role of the evolution of active regions in UV irradiance variability.

SINGLE VARIABLE LINEAR REGRESSION ANALYSIS

To reveal the correlation between Lyman alpha irradiance and solar activity indices, including total irradiance, we use simple linear regression analysis as a first step. The solar indices have been scaled to Lyman alpha by means of the equation: $y = a + b \times x$, where x is the selected solar index and y is the estimated Lyman alpha value. The a and b regression coefficients are calculated from the daily values of Lyman alpha and the different solar indices. Figs. 1(a-h) show the 27-day running means of Lyman alpha observed by the SME satellite (solid lines) and the results of the regressions (dashed lines) against S (a), Sc (b), F10 (c), CI (d), PI (e), EWHe (f), PSSA of active (g) and passive (h) spots. The correlation coefficients (r1) between the observed and estimated Lyman alpha flux values as well as the a and b regression coefficients are summarized in Table 1. The units of the selected solar indices are given in the footnote of Table 1. The Lyman alpha flux values are expressed in units of W/m^2.

Table 1

Results of simple and multiple linear regression analyses are summarized. The correlation coefficients (r1 and r2) calculated between the observed Lyman alpha and its estimations from the listed solar indices are given. The regression coefficients are also listed for both simple and multiple regressions.

Indices	Linear regression analyses						
	Single variable				Multiple		
	r1	a	b	r2	a	b	c
S	0.49	−1.0	7.7E−4	0.85	−2.8	3.4E−5	2.1E−3
Sc	0.91	−1.3	9.7E−4	0.94	−1.5	4.0E−4	6.9E−3
F10	0.90	3.2E−3	1.5E−5	0.92	3.0E−3	7.7E−6	9.1E−6
CI	0.91	3.7E−3	1.4E−4	0.93	3.6E−3	5.5E−7	1.0E−6
PI	0.85	4.2E−3	3.5E−5	0.91	4.1E−3	1.2E−5	3.4E−5
EWHe	0.96	1.4E−3	6.1E−5	0.96	1.4E−3	5.3E−5	8.7E−6
PSSA act	0.57	4.7E−3	3.6E−7	0.80	4.3E−3	7.4E−8	8.3E−7
PSSA pas	0.73	4.5E−3	9.8E−7	0.87	4.2E−3	1.3E−7	1.5E−6

units: S and Sc: W/m^2; F10: $10^{22}W/m^2/Hz$; CI: $10^{16}W/sr$; PI: 10^{-6} of the hemisphere; EWHe: mA; projected sunspots areas: 10^{-6} of the disk.

As can be seen from Fig. 1, the Lyman alpha fluxes estimated from various solar indices sometimes under-, sometimes overestimate its observed variability. The observed Lyman alpha generally decreases until mid-1986, when it reaches a minimum and begins to rise again. The Lyman alpha values estimated from S, Sc, F10, PI and PSSA tend to reach minimum levels in early 1985 and

then show flat backgrounds during the two years of minimum, with only small changes occurring on the solar rotational time scale. This behavior for F10 has already been shown by Barth et al.[2]. The Lyman alpha modeled from EWHe and CI shows behavior similar to the observed Lyman alpha, both with minima in mid-1986.

To study the variations of Lyman alpha we have subtracted the daily values of estimated Lyman alpha from the data to obtain the residuals plotted in Fig. 2(a-h). We have calculated power spectra for each of the residual time series. In order to concentrate on the high-frequency variability, these time series have been detrended by means of a 4th degree polynomial fit. The results of Fourier analysis are given in Fig. 3(a-h) for each residual. As can be seen from Figs. 2 and 3, the irradiance model based on EWHe gives the best fit with the Lyman alpha flux observed by the SME satellite. The power spectrum of the residuals for EWHe strongly resembles white noise, except for the low frequency domain (due to periods above 300-day). This and the high correlation (r1=0.96) between the observed Lyman alpha and its model based on EWHe shows that the full disk equivalent width of He 1083 is the best of these proxies for the UV irradiance.

The other residuals still show a significant variability. This indicates that S, Sc, F10, CI, PI, and PSSA are less reliable for modeling the UV irradiance with a single variable linear regression analysis. Finally, we note that Figs. 3(g) and 3(h) show quite different power spectra for residuals calculated from models based on PSSA of active and passive spots, respectively. Residuals from passive spot areas show more peaks, and this power spectrum is very similar to the power spectrum of projected areas of active spots (see Pap et al.[8]). Likewise, the power spectrum of residuals from active spot areas is very similar to the power spectrum of the projected areas of passive spots (shown in the paper of Pap et al.[8]). This shows that the developing complex active regions and the old decaying active regions cause strong, but qualitatively different signals in the UV irradiance. As Fig. 3(h) shows, in the remaining Lyman alpha variability, after removing the effect of old active regions, a strong 13.5-day period exists that is not present in the spectrum of residuals calculated from the active spot areas. This suggests that the 13.5-day periodicity of UV flux (e.g. Donnelly[9]) may tend to arise from the effect of developing complex regions, which are located in opposite hemispheres, as has been shown by Bai[10].

MULTIPLE LINEAR REGRESSION ANALYSIS

In order to improve the statistical models of Lyman alpha, multiple regression analysis has been used instead of single variable linear regression. The estimated Lyman alpha is now calculated from the equation: $y = a + b \times x + c \times z$, where a, b, and c are the partial regression coefficients (Table 1). x is the selected solar index and z is its 81-day running mean. The parameter b characterizes the variation related to the rapid fluctuations of the given index, while c describes the slower fluctuations seen in the 81-day smoothing. Therefore, y gives the best-fit relationship between Lyman alpha and solar activity indices, considering both the short- and long-term variabilities. The multiple correlation coefficients (r2) are listed in Table 1.

Figs. 4(a-h) show the 27-day running means of SME/Lyman alpha observations (solid lines) and Lyman alpha values estimated with multiple regression analysis from various solar indices (dashed lines). As can be seen, the correlation between the observed Lyman alpha and its models is improved significantly for the total irradiance and the projected sunspot areas. The correlation coefficients are also higher for the models calculated from Sc, F10, CI and PI. The residuals between the observed and modeled Lyman alpha values are calculated again and plotted in Figs.

5(a-h). After detrending these residuals by means of a 4th degree polynomial fit, we again Fourier-analyze them. The power spectra of these residual time series are shown in Figs. 6(a-h). Comparing Figs. 3 and 6, it can be seen that the power spectra of the remaining Lyman alpha flux are simplified in case of multiple regression analysis relative to that for the single variable linear regression. The main features of power spectra of these residuals are the clearly seen peaks at the rotational period and at 13.5-day, plus broad-band power below 0.1 micro Hz (periods > 100 days). Both of these features are minimal for the EWHe, again establishing it as the best proxy.

Figs. 4, 5, and 6, and Table 1 demonstrate that models of Lyman alpha developed with multiple regression analysis describe the observed irradiance variations better than models calculated with single variable linear regression analysis. Using multiple regression, the models fit reasonably well both the short- and long-term changes observed in Lyman alpha, with detailed differences in the magnitude of the rotational modulation relative to the slowly-varying components. In case of EWHe, the multiple regression analysis gives only a small improvement compared to the model calculated by a single variable linear regression. Table 1 shows that for EWHe the b partial regression coefficient is larger than c. This also shows that changes in the daily values of EWHe correlate better with the variation of Lyman alpha than the changes in the smoothed EWHe.

CONCLUSIONS

Our results demonstrate that models of Lyman alpha calculated with single variable linear regression analysis from various solar indices (other than the He 1083 nm line equivalent width) cannot describe totally the observed variations of Lyman alpha solar irradiance. These models under- or overestimate the short-term changes, and a phase shift is seen between the minimum times of Lyman alpha and its estimates from the total irradiance, total irradiance corrected for sunspot darkening, 10.7 cm radio flux, Ca-K plage index and projected sunspot areas. Multiple linear regression models predict much better both the short- and long-term variations observed in Lyman alpha, but still leave considerable power not modeled at the 27-day solar rotational and 13.5-day periods. In the case of the He 1083 nm line equivalent width the fits between the Lyman alpha values and their estimates are good using both single variable and multiple regression analyses. Residuals are of comparable size and both models explain about 92 percent of the variations observed in Lyman alpha irradiance.

Figs. 2 and 5 show a systematic variation of residuals, especially for the 10.7 cm radio flux and projected sunspot areas. This variation is caused by a phase shift between Lyman alpha and these solar indices used to produce the model, indicating their systematically different physical origin. The changes in the 10.7 cm radio flux and sunspot areas are related to the strong magnetic fields. Thus, their variation is the largest during the first appearance of magnetic fields on the solar disk. The plages are more long-lived than sunspots, and their area may be more extended during their second or third rotations than during their first appearance. This means that the peaks in the 10.7 cm radio flux caused by strong magnetic fields decrease faster than peaks in Lyman alpha which are caused mainly by plages. Our results also show that mainly during solar minimum, the plages themselves cannot account for the observed variations of UV irradiance. One may suppose that the plage remnants, which are neglected from the present Ca-K plage data (see Marquette and Martin[11]), influence the UV irradiance. This indicates the neccessity of improvements of the present UV-models (e.g. Lean and Skumanich[12]) by direct photometric observations of plages and

plage remnants. It is also shown that the evolution of active regions should be taken into account in the irradiance models. Until the time that new "photometric UV-models" are developed, the He-1083 nm line equivalent width can be used as the best proxy for the Lyman alpha irradiance.

ACKNOWLEDGEMENTS

REFERENCES

1. Lean, J., 'Solar UV variations', J. Geophys. Res. Vol. 92, 839-868, 1987.

2. Barth, C.A., Tobiska, W.K., and Rottman, G.A., 'Comparison of 10.7 cm radio flux with SME solar Lyman alpha flux', Geophys. Res. Let. (1990), in press.

3. Willson, R.C., 'Measurements of solar total irradiance and its variability', Space Sci. Rev. 38, 203-242, 1984.

4. Hudson, H.S., Silva, S., Woodard, M., and Willson, R.C., The effect of sunspots on solar irradiance, Solar Phys. 76, 211-219, 1982.

5. Rybansky, M., Rusin, V., and Dzifcakova, E., 'Coronal index of solar activity', Bull. Astron. Inst. Czechosl. 39, 106-119, 1988.

6. Harvey, J.W., 'Variation of the solar He I 10830 A line: 1977-1980', in Variations of the Solar Constant', (ed.) S. Sofia, NASA-2191, p. 265-272, 1980.

7. Pap, J., 'Variation of the solar constant during the solar cycle', Astrophys. Space Sci. 127, 55-71, 1986.

8. Pap, J., Tobiska, K., and Bouwer D., 'Periodicities of solar irradiance and solar activity indices I.', Solar Phys. in press, 1990.

9. Donnelly, R.F., 'Solar UV variability', in Proceedings of the IAGA Symposium for Solar Activity Forcing of the Middle Atmosphere, (ed.) J. Lastovicka, p. 1-8., 1989.

10. Bai, T., 'Distribution of flares on the Sun: superactive regions and active zones of 1980-1985', Ap.J. 314, 795-807, 1987.

11. Marquette, W.H., and Martin, S.F., Long-term evolution of a high-latitude active region, Solar Phys. 117, 227-241, 1988

12. Lean J., and Skumanich, A., 'Variability of the Lyman alpha flux with solar activity', J. Geophys. Res. 88, 5751-5759, 1983.
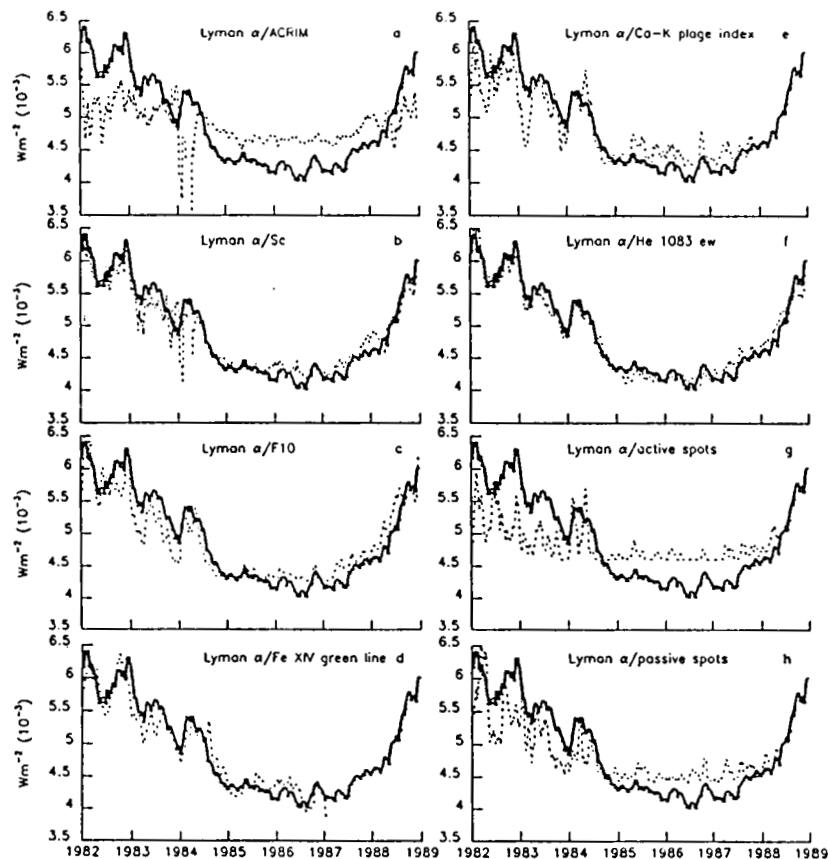
Fig. 1. Solid lines show the 27-day running means of SME Lyman alpha. Dashed lines show the 27-day running means of Lyman alpha estimated with simple linear regression analysis. The appropriate solar indices are printed on each plot.
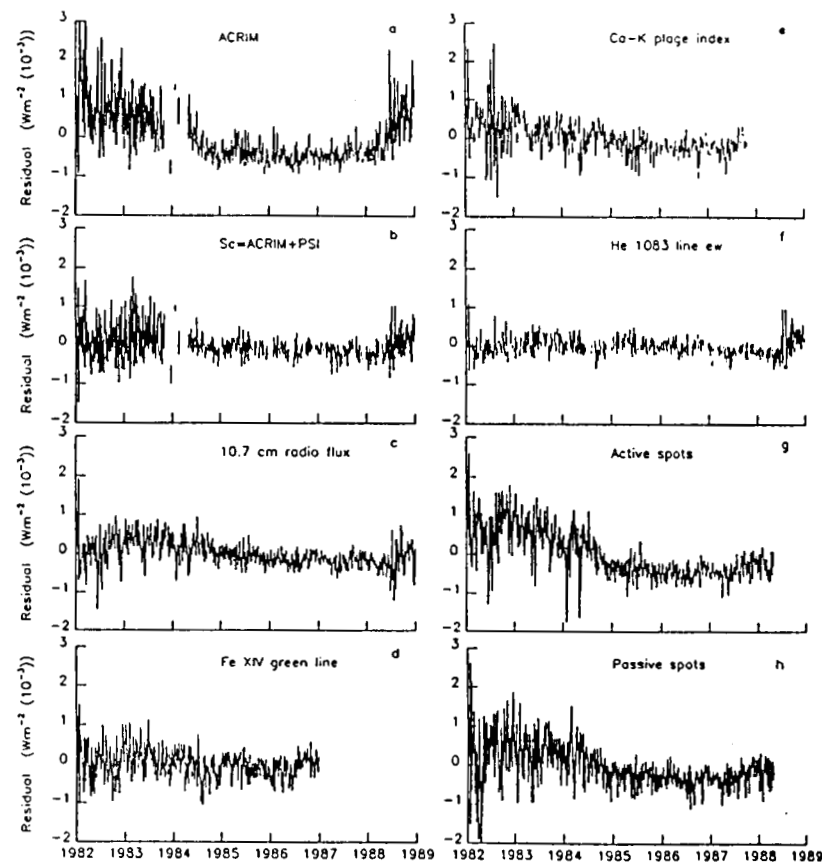
Fig. 2. The residuals after subtracting the daily values of Lyman alpha modeled with simple linear regression from the observed Lyman alpha data. The selected solar indices used for modeling are printed on each plot.
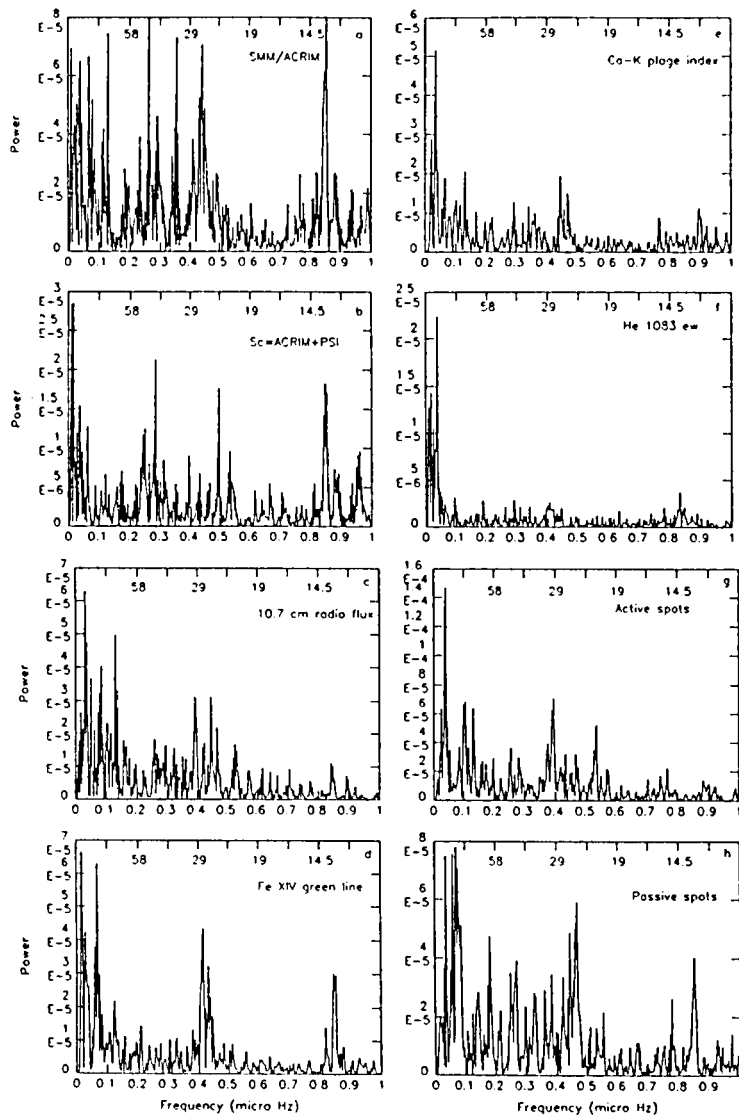
Fig. 3. Power spetra of residuals between the daily values of the observed Lyman alpha and Lyman alpha modeled with simple linear regression analysis. The solar indeces used for modeling Lyman alpha are printed on each spectrum. Periods in days are written on the top of the power spectra.
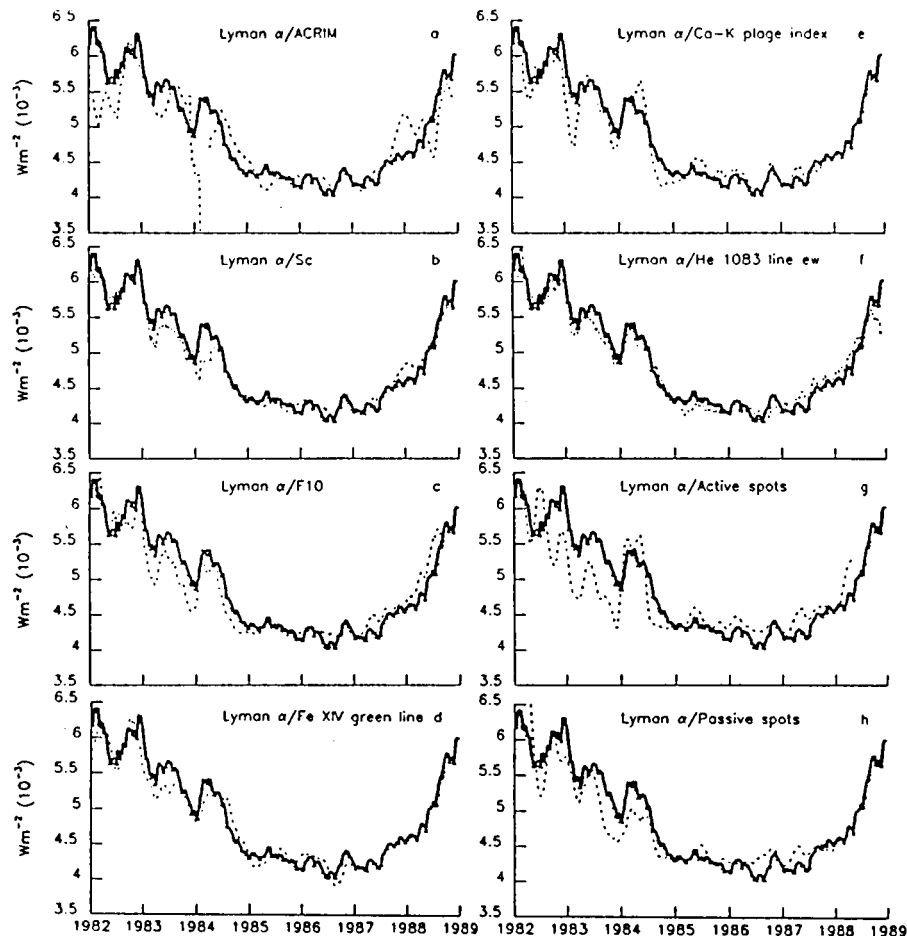

Fig. 4. Solid lines give the 27-day running means of SME Lyman alpha. Dashed lines show the 27-day running means of Lyman alpha modeled with multiple linear regression analysis. The selected solar indices used for modeling Lyman alpha are printed on each plot.
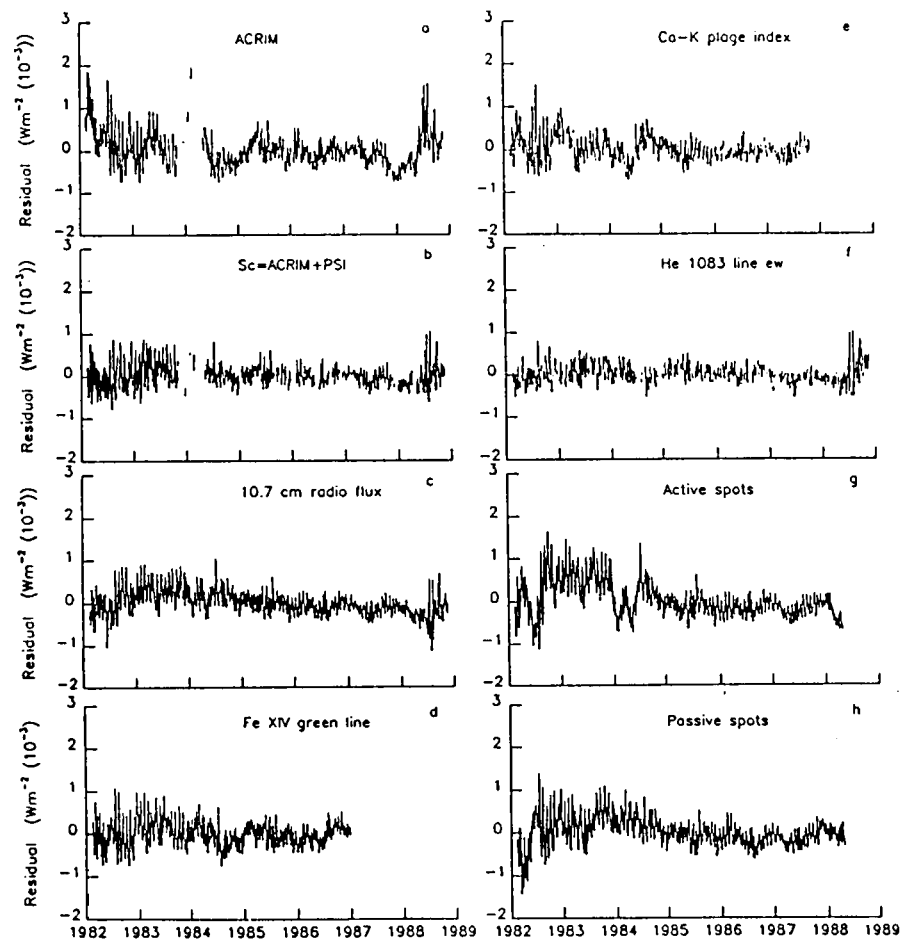
Fig. 5. The residuals between the daily values of the observed Lyman alpha and Lyman alpha modeled with multiple regression analysis are given. The solar indices selected for modeling Lyman alpha are printed on each plot.
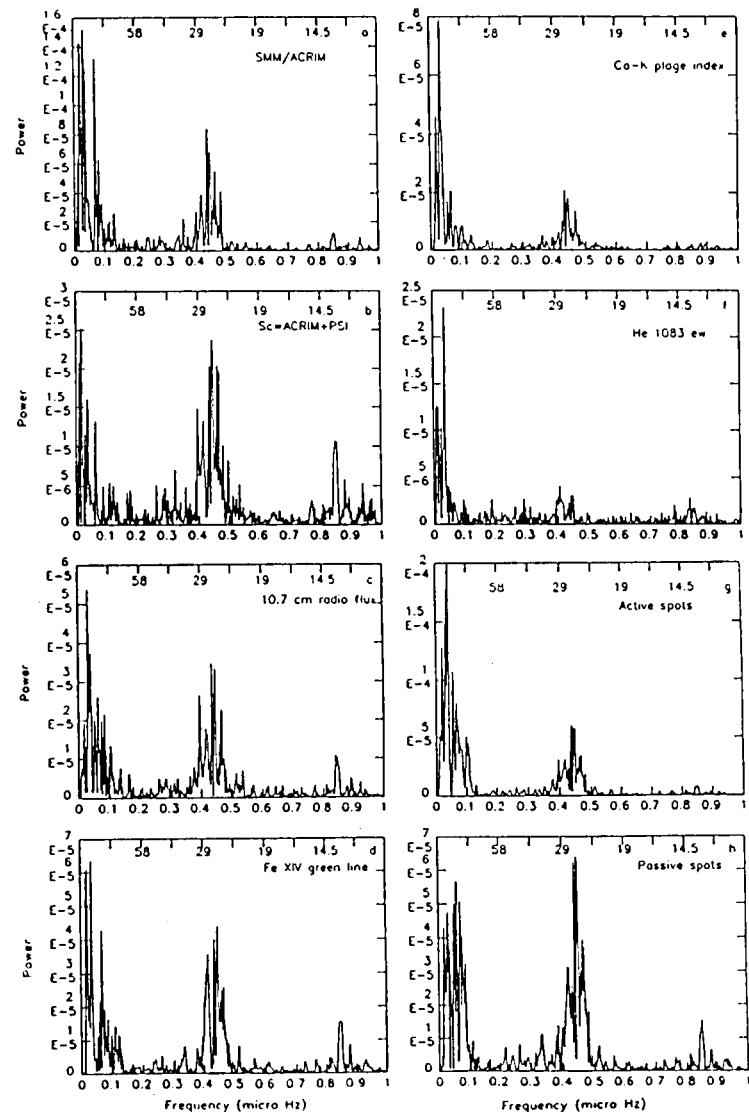

Fig. 6. Power spectra of residuals between the observed and modeled Lyman alpha values are given. Lyman alpha is modeled with multiple linear regression analysis. The appropriate solar indices used for modeling Lyman alpha are printed on each plot. The periods in days are also printed on each power spectrum.